Published in final edited form as:

*Oncogene*. 2019 January ; 38(5): 656–670. doi:10.1038/s41388-018-0482-y.

# Targeting the EMT transcription factor TWIST1 overcomes resistance to EGFR inhibitors in *EGFR*-mutant non-small cell lung cancer

**Zachary A. Yochum**[#1,2], **Jessica Cades**[#3,5], **Hailun Wang**[#4], **Suman Chatterjee**[2], **Brian W. Simons**[7], **James P. O'Brien**[2], **Susheel K. Khetarpal**[2], **Ghali Lemtiri-Chlieh**[4], **Kayla V. Myers**[2], **Eric H.-B. Huang**[2], **Charles M. Rudin**[6], **Phuoc T. Tran**[4,5,7,#], and **Timothy F. Burns**[1,2,#]

[1]Department of Pharmacology and Chemical Biology, University of Pittsburgh, Pittsburgh, PA

[2]Department of Medicine, Division of Hematology-Oncology, UPMC Hillman Cancer Center, Pittsburgh, PA.

[3]Department of Pharmacology, Sidney Kimmel Comprehensive Cancer Center, Johns Hopkins University School of Medicine, Baltimore, MD.

[4]Department of Radiation Oncology and Molecular Radiation Sciences, Sidney Kimmel Comprehensive Cancer Center, Johns Hopkins University School of Medicine, Baltimore, MD, USA

[5]Department of Oncology, Sidney Kimmel Comprehensive Cancer Center, Johns Hopkins University School of Medicine, Baltimore, MD, USA

[6]Department of Medicine, Thoracic Oncology Service, Memorial Sloan Kettering Cancer Center, New York, NY.

[7]Department of Urology, Johns Hopkins University School of Medicine, Baltimore, MD

[#] These authors contributed equally to this work.

## Abstract

Patients with *EGFR*-mutant non-small cell lung cancer (NSCLC) have significantly benefited from the use of EGFR tyrosine kinase inhibitors (TKIs). However, long-term efficacy of these therapies is limited due to *de novo* resistance (~30%) as well as acquired resistance. Epithelial-mesenchymal transition transcription factors (EMT-TFs), have been identified as drivers of EMT-mediated resistance to EGFR TKIs, however, strategies to target EMT-TFs are lacking. As the third-generation EGFR TKI, osimertinib, has now been adopted in the first-line setting, the frequency of *T790M* mutations will significantly decrease in the acquired resistance setting.



**Corresponding authors:** Phuoc T. Tran, M.D./Ph.D., Sidney Kimmel Comprehensive Cancer Center, Johns Hopkins Hospital, 1550 Orleans Street, CRB2 Rm 406, Baltimore, MD 21231. Phone: 410-614-3880; Fax: 410-502-1419; tranp@jhmi.edu. Timothy F. Burns, M.D./Ph.D., UPMC Hillman Cancer Center, Hillman Cancer Center Research Pavilion, Office: Suite 2.18e Lab: 2.7, 5117 Centre Avenue, Pittsburgh, PA 15213-1863; Phone: 412-864-7859; Fax: 412-623-7768; burnstf@upmc.edu. [#]denotes co-corresponding authors.

Disclosure of Potential Conflicts of Interest

No potential conflicts of interest were disclosed.

Previously less common mechanisms of acquired resistance to 1st generation EGFR TKIs including EMT are now being observed at an increased frequency after osimertinib. Importantly, there are no other FDA approved targeted therapies after progression on osimertinib. Here, we investigated a novel strategy to overcome EGFR TKI resistance through targeting the EMT-TF, TWIST1, in *EGFR*-mutant NSCLC. We demonstrated that genetic silencing of *TWIST1* or treatment with the TWIST1 inhibitor, harmine, resulted in growth inhibition and apoptosis in *EGFR*-mutant NSCLC. TWIST1 overexpression resulted in erlotinib and osimertinib resistance in *EGFR*-mutant NSCLC cells. Conversely, genetic and pharmacological inhibition of TWIST1 in EGFR TKI resistant *EGFR*-mutant cells increased sensitivity to EGFR TKIs. TWIST1-mediated EGFR TKI resistance was due in part to TWIST1 suppression of transcription of the pro-apoptotic BH3-only gene, *BCL2L11* (BIM), by directly binding to *BCL2L11* intronic regions and promoter. As such, pan-BCL2 inhibitor treatment overcame TWIST1-mediated EGFR TKI resistance and were more effective in the setting of TWIST1 overexpression. Finally, in a mouse model of autochthonous *EGFR*-mutant lung cancer, Twist1 overexpression resulted in erlotinib resistance and suppression of erlotinib-induced apoptosis. These studies establish TWIST1 as a driver of resistance to EGFR TKIs and provide rationale for use of TWIST1 inhibitors or BCL2 inhibitors as means to overcome EMT-mediated resistance to EGFR TKIs.

**Keywords**

EGFR; TWIST1 inhibitor; lung cancer; EMT; BIM

## INTRODUCTION

Lung cancer remains the leading cause of cancer related mortality in the United States and worldwide. Despite a 15% five-year survival rate, there have been improvements in the treatment of subsets of non-small cell lung cancer (NSCLC) patients with known targetable molecular drivers such as mutations in *EGFR*, *BRAF* and *MET*, and translocations involving *ALK, ROS1, RET and NTRK1/2* (1–3). Previous studies have demonstrated that patients with *EGFR*-mutant tumors (~15%) can have marked responses to EGFR tyrosine kinase inhibitors (TKIs). While approximately 70% of patients demonstrate responses to such therapies, long-term efficacy of these therapies is limited due to the inevitability of acquired resistance and frequent *de-novo* resistance (~30%) (4–6). Efforts to identify drivers of acquired resistance to first generation EGFR TKIs have revealed multiple mechanisms of resistance including *T790M* gatekeeper *EGFR* mutations (~49%), *MET* amplification (~5%), conversion to small-cell lung cancer (~14%), and *PIK3CA* mutations (~5%) (7).

In as many as 20% of patients, resistance to EGFR TKIs including third generation inhibitors, such as osimertinib, is associated with an epithelial-mesenchymal transition (EMT) phenotype (7–10). EMT is a reversible process of transdifferentiation in which epithelial cells lose their polarity and cell-cell interactions and adopt a mesenchymal phenotype (11, 12). This process is associated with a variety of pro-tumorigenic functions such as with increased invasion, metastasis, and suppression of failsafe programs of apoptosis and senescence (11, 12). Interestingly, the presence of an EMT or mesenchymal phenotype is associated with both *de-novo* as well as acquired resistance to EGFR TKIs (7,

13–15). Previous studies have demonstrated that upregulation of AXL, TFG-β, and IGF1R signaling axes are drivers of EMT-mediated acquired resistance to EGFR TKIs (8, 16–18). Recent studies have implicated EMT transcription factors (EMT-TFs), which are drivers of global transcriptional changes that lead to EMT, in resistance to targeted therapies in *EGFR*-mutant NSCLC (19). Specifically, upregulation of the EMT-TFs, SNAI2 and ZEB1, have been shown to can confer resistance to EGFR TKIs (20–22). However, the mechanism(s) by which these EMT-TFs mediate resistance and therapeutic strategies to target these EMT-TFs have been lacking.

We have previously demonstrated that the EMT-TF, TWIST1, is required for oncogene-driven NSCLC (23). In multiple oncogene-driver dependent settings, including tumors with *EGFR* mutations, TWIST1 functions to suppress oncogene-induced senescence and apoptosis (23–25). In addition to suppressing failsafe programs, TWIST1 has also been shown to promote EMT, metastasis, and therapeutic resistance (26–29). We have also identified a first-in-class inhibitor of TWIST1, harmine that has significant anti-tumor activity in oncogene driver dependent NSCLC including *EGFR*-mutant NSCLC (25). In the current study, we demonstrated genetic and pharmacological inhibition of TWIST1 resulted in growth inhibition and apoptosis in *EGFR*-mutant NSCLC cell lines, including cells with acquired resistance *T790M* mutations. We also identified TWIST1 as a driver of resistance to EGFR TKIs in EGFR TKI naïve *EGFR*-mutant NSCLC cell lines as well as in EGFR TKI acquired resistant cell lines with *T790M* mutations. We further demonstrated that TWIST1 is able to mediate resistance in a transgenic mouse model of autochthonous *EGFR*-mutant lung cancer. We have identified that one mechanism by which TWIST1 mediates resistance is through suppression of EGFR TKI-induced apoptosis by directly binding to the promoter and intronic regions of the pro-apoptotic BH3-only gene, *BCL2L11* (BIM) and repressing BIM transcription. Additionally, we demonstrated that TWIST1-mediated EGFR TKI resistance can be overcome with either a BCL-2/BCL-XL inhibitor, or the TWIST1 inhibitor harmine, suggesting that targeting TWIST1 in the clinic may be a viable option to overcome EMT-mediated resistance to EGFR TKIs.

## RESULTS

### Genetic or pharmacologic Inhibition of TWIST1 results in growth inhibition and apoptosis in *EGFR*-mutant NSCLC

We previously observed that TWIST1 expression is required for tumorigenesis in oncogene-driven NSCLC as inhibition of *TWIST1*, in oncogene driver dependent NSCLC cell lines, results in activation of latent senescence and/or apoptotic programs (23–25). To more comprehensively test the role of TWIST1 in *EGFR*-mutant lung cancers, we first assessed relative expression of TWIST1 in a panel of *EGFR*-mutant NSCLC cell lines with TKI sensitizing mutations such as the *L858R* mutation and Exon 19 deletions and *EGFR*-mutant NSCLC cell lines with the EGFR TKI acquired resistance *T790M* mutation (Figure 1a). TWIST1 was broadly expressed across both EGFR TKI sensitive and resistant cell lines (Figure 1a). Of note, we identified an *EGFR*-mutant cell line, H1650, previously demonstrated to have de-novo resistant to EGFR TKIs (30) had increased levels of TWIST1 mRNA and protein. Next, we infected the panel of *EGFR*-mutant lines with shRNAs

targeting *TWIST1* or with scrambled control shRNA. Genetic inhibition of *TWIST1* inhibits growth in the majority of lines screened (Figure 1b). We have previously identified and characterized a novel TWIST1 inhibitor, harmine, that had anti-cancer activity in oncogene driver defined NSCLCs, inhibited multiple TWIST1-dependent functions, and induced degradation of TWIST1 (25). Similar to our previous findings in a limited number of *EGFR*-mutant cell lines, harmine markedly inhibited growth across the large panel of *EGFR*-mutant NSCLC cell lines, including EGFR TKI resistant lines, similar to the effects seen following silencing of *TWIST1* (Figure 1b). While we have previously observed that genetic and pharmacological inhibition of TWIST1 primarily results in oncogene-induced senescence (OIS) (23–25), there was a subset of cell lines that appeared more dependent on TWIST1 expression for survival and underwent apoptosis following inhibition of TWIST1 (23, 25). We identified a subset of *EGFR*-mutant cell lines (H1975 and PC9) that underwent apoptosis following knockdown of TWIST1 and harmine treatment (Figure 2a-b, Supplementary Figure 1). PC9 cells have an EGFR TKI sensitizing EGFR exon 19 deletion (ΔE746-A750) and H1975 cells have both EGFR TKI sensitizing *L858R* mutation and an acquired resistance *T790M* mutation, suggesting that targeting TWIST1 may be an effective therapeutic target for *EGFR*-mutant disease in both the EGFR TKI naïve and EGFR TKI acquired resistance setting. Of note, genetic and pharmacologic inhibition of TWIST1 (Figure 1b) was also effective in the setting of *T790M* independent resistance such as in the EGFR TKI resistant cell line H1650 (30).

## TWIST1 is necessary and sufficient for EGFR TKI resistance in a subset of *EGFR*-mutant NSCLC cell lines

Recent evidence has suggested that EMT-TFs mediate resistance to EGFR targeted therapy in lung cancer (20–22, 31). TWIST1 has been implicated in chemoresistance in lung cancer and other cancer types (27, 32–34). Given the requirement of TWIST1 for *EGFR*-mutant NSCLC and its role in suppressing OIS and apoptosis in NSCLC, we investigated whether enforced TWIST1 expression would be sufficient to cause resistance to EGFR TKIs, using a panel of doxycycline inducible TWIST1 overexpressing *EGFR*-mutant NSCLC cell lines. TWIST1 overexpression in these lines was sufficient to cause resistance to both 1$^{st}$ and 3$^{rd}$ generation EGFR TKIs (Figure 3 and Supplementary Figure 2). Additionally, we observed that TWIST1-mediated resistance was associated with suppression of EGFR TKI-induced apoptosis in cells with and without the *T790M EGFR* gatekeeper mutation (Supplementary Figure 2).

To investigate the requirement of TWIST1 for erlotinib resistance, we assessed whether genetic or pharmacologic inhibition of TWIST1 in *EGFR*-mutant TKI resistant cell lines could restore sensitivity to EGFR TKIs. As demonstrated in Figure 1a, we identified that the EGFR-mutant cell line, H1650 had increased levels of TWIST1 mRNA and protein. Interestingly, this cell line demonstrates *de-novo* resistance to EGFR TKIs (30). We found that genetic silencing of *TWIST1* increases sensitivity of this cell line to erlotinib (Figure 4a). We observed a similar increase of sensitivity to erlotinib when used in combination with our small molecule TWIST1 inhibitor, harmine (Figure 4b). This increase in erlotinib sensitivity corresponded to increased apoptosis and expression of BIM, a pro-apoptotic BH3 protein shown to be critically important for response to EGFR TKIs (35). As such, BIM

expression increased with decreased TWIST1 expression following harmine and erlotinib co-treatment (Figure 4b). Of note, the combination of harmine and erlotinib results in an approximate 2–2.2 fold increase in BIM expression, which suggests that upregulation of BIM may be a mechanism by which inhibition of TWIST1 increases EGFR TKI sensitivity (Supplementary Figure 3a). We next investigated the role of TWIST1 in mediating resistance in an *EGFR*-mutant NSCLC cell line (HCC827R2) with acquired resistance to erlotinib (36). Although TWIST1 was not increased in the resistant cell line compared to the parental cell line, we observed that this cell line maintained a requirement for TWIST1 expression and that targeting TWIST1 in these cells increased sensitivity to erlotinib (Supplementary Figure 3b-c). These observations indicate that inhibiting TWIST1 may be a viable target in the erlotinib resistance settings in which TWIST1 is expressed.

## TWIST1 suppresses BIM expression

Previous studies have established that response to oncogene targeted therapies requires BIM expression and loss of BIM expression is associated with EGFR TKI resistance in patients (35–39). BIM expression is regulated both transcriptionally and post-translationally (40). We investigated whether TWIST1 could regulate BIM expression in *EGFR*-mutant NSCLC cell lines. We found that knockdown of *TWIST1* resulted in increased *BCL2L11* (BIM gene) mRNA and protein expression of BIM (Figure 5a). In the cell lines in which TWIST1 was sufficient to mediate erlotinib resistance, we demonstrated that TWIST1 overexpression resulted in suppression of the mRNA and protein expression of BIM (Figure 5b-c). To evaluate whether TWIST1 decreased BIM expression through a post-translational mechanism, we performed a pulse-chase experiment and demonstrated that TWIST1 did not decrease BIM half-life, suggesting that TWIST1 negative regulation of BIM expression is primarily at the mRNA level (Supplementary Figure 4). To explore whether TWIST1 was directly repressing the transcription of *BCL2L11*, we performed TWIST1 ChIP on the promoter region and intron 1 which contained multiple E-box binding sites (CANNTG), the putative consensus binding site for TWIST1. We also performed TWIST1 ChIP on a potential TWIST1 binding site contained within the *BCL2L11* genomic region in intron 12 previously identified as a putative binding sequence from a global TWIST1 ChIP analysis (41). We identified that TWIST1 bound to one site upstream of the transcriptional start site (BS1) and a site in intron 12 (BS5) (Figure 5d). These studies establish BIM as a novel target gene of TWIST1. While others have previously established the requirement of BIM for response to EGFR TKIs (35, 37–39), we confirmed that in H1975 cells that BIM expression was required for response to osimertinib (Figure 5e). As BIM appeared to be required for EGFR TKI induced apoptosis we examined whether inhibition of anti-apoptotic BCL2 family members with the BCL-2/BCL-XL inhibitor (ABT-737) would be effective in TWIST1 overexpressing *EGFR*-mutant NSCLC. We observed that BCL2/BCLXL inhibitor (ABT-737) was able to overcome TWIST1-mediated resistance to osimertinib in H1975 TWIST1 overexpression cells (TWIST1-ON) but did not affect osimertinib sensitivity in the absence of TWIST1 (TWIST-OFF) (Figure 5f). These data suggest that TWIST1-mediated resistance may be overcome through use of BH3 mimetics and that these therapies may be more effective in TWIST1 overexpressing *EGFR*-mutant NSCLC cells.

## Creation and Characterization of an Autochthonous *EGFR*-Mutant *Twist1* Overexpressing Lung Tumor Mouse Model

We previously demonstrated that *Twist1* could cooperate with mutant *Kras* for lung tumorigenesis and that genetic or pharmacologic inhibition of Twist1 in this model inhibited growth of these lung tumors (23–25). To investigate whether EMT and Twist1 could impart erlotinib resistance to *EGFR*-mutant NSCLCs *in vivo* we made use of transgenic $EGFR^{L858R}$ and *Twist1* inducible mouse models (24, 42). Both of these strains are well established doxycycline inducible lung specific transgenic mouse models: *CCSP-rtTA*/*tetO-*$EGFR^{L858R}$ (CE), expressing human $EGFR^{L858R}$ and *CCSP-rtTA*/*Twist1-tetO7-luc* (CT), expressing mouse *Twist1*. We crossed these two lines to create triple transgenic mice, *CCSP-rtTA*/*tetO-*$EGFR^{L858R}$/*Twist1-tetO7-luc* (CET) (Supplementary Fig. 5a). Cohorts of CE and CET mice, aged 4–8 weeks, were administered doxycycline in the drinking water to turn on the transgenes. After 4 weeks, a point by which CE mice were reported to develop lung tumors (42), mice were sacrificed and necropsies performed. Upon comparison of H&E lung sections from CE and CET mice by a veterinary pathologist, both genotypes resulted in similarly diffuse adenocarcinoma growth in both lungs, as had been previously published for the CE model (42), but CET tumors were more anaplastic and had larger, more irregular nuclei (Supplementary Fig. 5b). We had previously shown that Twist1 expression accelerates mutant *Kras* tumorigenesis (24), but after 4 weeks on doxycycline, tumor burden was similar between CE and CET mice as shown by pathologic assessment of lung tumor burden (0 meaning no hyperplasia and 5 meaning >75% of the lung was affected) and microCT (Supplementary Figure 5b-c). Thus, TWIST1 expression did not appear to have a primary effect on tumor proliferation rate, but rather resulted in a more aggressive or anaplastic appearance in the CET tumors.

To further characterize the novel CET mouse model, we looked at levels of epithelial and mesenchymal markers. We immunostained lung sections from both CE and CET mice with antibodies for E-cadherin, an epithelial marker, and vimentin, a mesenchymal marker. There was no distinguishable difference in levels of either marker between CE and CET mice (Supplementary Figure 5d). We also did not observe any increased metastasis in the CET mice. In other contexts, Twist1 has been shown to impact the proliferation rate of tumor cells as well as apoptosis levels (23, 43). We next examined the levels of proliferation through Ki-67 staining and apoptosis with cleaved caspase 3 staining. The overexpression of Twist1 in CET mice in fact modestly decreased proliferation rates, as measured by Ki-67 IHC, in comparison to CE mice (Supplementary Figure 5e). There was no significant effect on apoptosis with Twist1 expression (Supplementary Figure 5f).

### *Twist1* expression induces erlotinib resistance *in vivo*.

After characterizing the novel CET mouse model in the absence of drug treatment, we investigated whether Twist1 expression could induce resistance to the EGFR TKI erlotinib *in vivo*. As previously described, upon administration of erlotinib to CE mice, most lung tumors regress, with a distribution of objective responses including disease stabilization, partial response, and complete response (42). In order to compare CE and CET mice tumor responses and overall survival, all mice were put on doxycycline, to turn on transgene expression and allowed to develop tumors for 3 weeks. Both CE and CET mice had similar

levels of tumor burden prior to the start of treatment. At that time point, treatment day 0, all mice were scanned by microCT and this scan was used as the baseline. The mice were treated for 3 weeks with erlotinib and scanned by microCT each week (Figure 6a). When baseline scans were compared to scans from after 3 weeks of erlotinib treatment, tumor regression was clearly visible in CE mice, while CET mice showed an increase in tumor burden (Figure 6b). All scans were assessed and tumor burden graded on a scale of 0 (no tumor visible) to 5 (lungs completely filled with tumor). Based on the tumor burden change from the beginning to the end of treatment, a majority of CE mice demonstrated no disease progression with erlotinib, with no progression including complete and partial responses as well as stable disease. Conversely, over half of the CET mice had tumor progression over the three weeks of treatment (Figure 6c). When examining erlotinib treatment responses based on degree of lung tumor regression, two-thirds of CE mice showed lung tumor regression, while only a quarter of CET mouse lung tumors regressed (Figure 6c). After the 3 weeks of treatment, mice were monitored for weight loss, lethargy and other signs indicating a need for euthanasia. CET mice median overall survival time from the beginning of treatment was 6.8 weeks, while CE mice lived a median of 8.7 weeks (Figure 6d). Importantly, we have demonstrated that Twist1 expression does not lead to an increased tumor burden in the *EGFR*-mutant background so an increased tumor burden cannot explain this decrease in overall survival (Figure 6d). These data support that expression of Twist1 in CET mice induces resistance to erlotinib as shown by increased lung tumor burden by microCT and decreased overall survival time following treatment with erlotinib.

To confirm the differences seen by microCT, a cohort of CE and CET mice were treated with erlotinib for 1 week followed by euthanasia for macroscopic and histologic tumor assessment. While partial and complete responses were seen in CE mice, only partial and no responses occurred in the CET mice (Figure 7a). Tumor burden as assessed on H&E slides by a veterinary pathologist between CE and CET mice treated with erlotinib demonstrated an early trend towards CET mice having greater tumor burden at 1 week (Figure 7a).

We then examined the mechanism of Twist1-mediated resistance. Since Twist1 is one of the key mediators of EMT, the tumor cells could be undergoing this phenotypic change. However, staining for E-cadherin and vimentin showed no change with Twist1 expression, with or without erlotinib treatment (Figure 7b). Additionally, there was no significant difference between proliferation levels in CE and CET mice following erlotinib treatment (Figure 7c). Interestingly, when the amount of apoptosis was assessed through staining for cleaved caspase 3, the levels of apoptosis were decreased in CET erlotinib treated lung tumors compared to CE erlotinib treated lung tumors (Figure 7c). These data suggest that while the level of proliferation and EMT status is unchanged following erlotinib treatment, Twist1 expression inhibits apoptosis in *EGFR*-mutant lung tumors following erlotinib treatment. Of note, we also examined Twist1 expression in residual tumors in CE mice following erlotinib treatment. Interestingly, we demonstrated that despite not expressing Twist1 at baseline, Twist1 was upregulated following erlotinib treatment in a subset of residual CE tumors (Supplementary Figure 6a). In addition, in CE tumors with Twist1 upregulation post-erlotinib treatment, cleaved caspase-3 was not expressed (Supplementary Figure 6b). While this is correlative data, it is consistent with our evidence that Twist1 is a mediatory of EGFR TKI resistance by suppressing EGFR TKI-induced apoptosis.

## DISCUSSION

We have previously demonstrated that TWIST1 expression is required for oncogene-driven tumorigenesis and that loss of TWIST1 expression results in activation of latent senescence and/or apoptotic programs. Here, we demonstrated that both genetic silencing and pharmacological inhibition of TWIST1 results in growth inhibition in a large panel of *EGFR*-mutant cell lines. Additionally, we identified that in a subset of *EGFR*-mutant cell lines inhibition of TWIST1 results in induction of apoptosis. Of note, targeting TWIST1 resulted in growth inhibition in cells with *EGFR* TKI sensitizing mutations and acquired resistance *T790M* mutations, suggesting that targeting TWIST1 may be a viable option in *EGFR*-mutant NSCLC both in the treatment naïve and acquired resistance settings.

Recently, others have demonstrated that EMT-TFs, specifically ZEB1 and SLUG, can contribute to resistance to EGFR TKIs (18–20). Hwang et. al have recently shown that TWIST1 overexpression is sufficient to cause EGFR TKI resistance in a single erlotinib sensitive cell line in long term assays and that VGF regulates TWIST1 (35). Here, we significantly expand upon these studies by demonstrating that TWIST1 overexpression is sufficient to cause resistance to EGFR TKIs, in multiple *EGFR*-mutant cell lines with and without *T790M* mutations. We also establish that Twist1 overexpression promotes erlotinib resistance *in vivo*, using a mouse model of autochthonous *EGFR*-mutant Twist1 overexpressing lung cancer. In both *EGFR*-mutant NSCLC cell lines and our mouse model of *EGFR*-mutant lung cancer, Twist1 overexpression was associated with suppression of EGFR TKI-induced apoptosis.

Importantly, as the third-generation EGFR TKI, osimertinib, has now been adopted in the first line setting (44), the frequency of T790M mutations will likely significantly decrease in the acquired resistance setting (44, 45). Previously uncommon mechanisms of resistance have already been observed at increased frequency after osimertinib including *MET* and *HER2* amplifications, *KRAS* mutations, additional second site *EGFR* mutations, EMT and SCLC transformation (44–51). Of note, there are no other FDA approved targeted agents for after progression on osimertinib (45). Thus, there is clearly a need for the development of novel targeted agents to prevent and overcome EGFR TKI resistance.

Our study is the first to establish that TWIST1 expression is required for resistance in *EGFR*-mutant cells that demonstrate *de-novo* or acquired resistance to EGFR TKIs. Importantly, our study demonstrates that therapeutic targeting of an EMT-TF, is able to restore sensitivity to erlotinib in *EGFR*-mutant NSCLC cells that are resistant to EGFR TKIs. Our findings suggest that use of small molecule compounds that inhibit TWIST1 may be a viable option to overcome *de-novo* and acquired resistance to EGFR TKIs in lung cancer. Harmine is an active β-carbolin alkaloid found in the herb *Peganum harmala* used in traditional medicine in Central Asia and the Middle East (52). However, in mouse model systems and in humans, the harmine therapeutic efficacy may be limited due to neurotoxic side effects, such as tremors (52, 53). We have identified analogues of harmine that are potentially more potent inhibitors of TWIST1 without the neurotoxicity associated with harmine and are currently performing further preclinical evaluation of these compounds.

Others have previously demonstrated that BIM expression is required for response to EGFR TKIs (35, 37–39). Additionally, BIM polymorphisms which result in decreased expression of functional BIM protein, are associated with resistance to EGFR TKIs (32, 54, 55). Here, we establish that TWIST1 suppresses BIM expression through direct binding at both the promoter and intronic regions. Overall, these data suggest that one of the mechanisms by which TWIST1 mediates EGFR TKI resistance is through inhibition of EGFR TKI-induced apoptosis by suppression of BIM expression. Interestingly, we demonstrated that TWIST1-mediated resistance can be overcome with use of BCL2/BCLxL inhibitors. BCL2/BCLxL inhibitors, such as ABT-263 are in clinical trials, and our data suggest that use of these inhibitors may provide rapid means to overcome TWIST1-mediated resistance in the clinic. While we established that one mechanism by which TWIST1 can mediate resistance is through suppression of apoptosis, TWIST1 has been previously shown to suppress senescence in both oncogene-driven NSCLC and breast cancer (23, 24, 56). We are currently exploring whether TWIST1 mediated suppression of senescence is potentially another mechanism by which TWIST1 promotes EGFR TKI resistance. Of note, a recent study demonstrated that TWIST1 can mediate resistance to 3$^{rd}$ generation EGFR TKIs through upregulation of the EMT-TF, ZEB1 (9). This study established that ZEB1 can also directly suppress *BCL2L11* transcription (9). This study and our current study suggests that there are potentially multiple mechanisms by which TWIST1 can promote EGFR TKI resistance and multiple mechanisms by which TWIST1 can suppress BIM expression.

In summary, we demonstrated that genetic and pharmacological inhibition of TWIST1 results in growth inhibition in *EGFR*-mutant NSCLC. In a subset of cell lines, including cell lines with acquired resistance *T790M* mutations, inhibition of TWIST1 is associated with the induction of apoptosis. Additionally, we established that TWIST1 is both sufficient and, in some lines, required for EGFR TKI resistance in *EGFR*-mutant NSCLC both *in vitro* and *in vivo*. We demonstrated that one of the mechanisms by which TWIST1 mediates resistance is through suppression of apoptosis via suppression of BIM expression. We also demonstrated that use of a TWIST1 inhibitor, harmine, was able to overcome both *de-novo* and acquired resistance to EGFR TKIs. Of note, targeting TWIST1 may be associated with minimal side effect because it is rarely expressed post-natally (57, 58). Our data suggests that targeting TWIST1 may be option to overcome EGFR TKI resistance in *EGFR*-mutant NSCLCs both in the *de-novo* and acquired resistance settings.

## METHODS

### Cell lines and Reagents

PC9, H1975, H1650, Hcc4006, Hcc4011, Hcc2935, Hcc827, H3255, and HEK 293T were acquired from the American Type Culture Collection (ATCC) and were cultured in the recommended ATCC media. Hcc827R2 and 11–18 cells were obtained from Dr. Christine Lovly (Vanderbilt University) and cultured in the recommended media. The identity of the aforementioned cell lines was verified by autosomal STR (short tandem repeat) profiling done at University of Arizona Genetics Core (UAGC). Mycoplasma testing was performed every six months using MycoAlert Detection Kit (Lonza). Osimertinib and erlotinib were

purchased from Selleck Chemicals (Houston, TX). Harmine was purchased from Sigma-Aldrich (St. Louis, MS). ABT-737 was purchased from ApexBio Technology (Houston, TX)

### CellEvent™ Caspase-3/7 Green Flow Cytometry

Cells were seeded at appropriate density in 25-$cm^2$ plates and incubated for 24 hours. Following incubation, cells were treated with harmine at 0, 20, 40μM for 48 hours. Apoptosis was analyzed as previously described (25).

### Quantitative RT-PCR

RNA isolation, cDNA generation, PowerUp™ SYBR® Green Master Mix (Perkin Elmer Applied Biosystems) and TaqMan® Universal PCR Master Mix (Perkin Elmer Applied Biosystems) were utilized as previously described (25). List of primers is provided in Supplementary Table 1–2.

### Cell proliferation assays

For all viability experiments, cells were seeded at an appropriate density in 96 well plates and incubated for 24 hours. Cells were subsequently treated with a range of doses of the appropriate inhibitor for 72 hours. Viability was determined using the CellTiter96® Aqueous One Solution Cell Proliferation Assay kit (Promega) or Cell-Titer Glo 2.0 Assay (Promega) according to manufacturer's protocol. Data was analyzed as previously described (25). To ensure consistent and reproducible results, experiments were performed at least twice.

### Western blot and antibodies

Following appropriate treatment, cells were harvested and lysed and subsequent protein was quantified and western blotting was performed as previously described (23). All information on antibodies is included in Supplementary Table 3.

### Chromatin Immunoprecipitation

H1975 TRE3G-TWIST1 cells were seeded in 15cm dishes and incubated for 24 hours. Cells were treated with 50ng/ml of doxycycline. Following 24 hours of doxycycline treatment, cells were harvested and Chromatin Immunoprecipitation (ChIP) assays were performed utilizing the SimpleChIP Enzymatic Chromatin IP Kit (Cell Signaling Technology) according to manufacturer's recommendations. ChIP primers that were used are included in Supplementary Table 4. For ChIP, 2μg of ChIP-grade TWIST1 antibody (Abcam, Ab5087) and 2μg Mouse IgG, Whole Molecule Control (Thermo Scientific, 31903) were used.

### Lentiviral cDNA and shRNA production

HEK 293T cells were seeded at a density of 4 X $10^6$ in 25-$cm^2$ flasks. Following a 24 hour incubation period, cells were transfected to generate lentivirus as previously described (23, 59). A complete list of the constructs used is provided in Supplementary Tables 5–7 and sequences are available upon request.

### Transgenic mice

Animals were housed in a pathogen free facility and all studies were approved by The Johns Hopkins University IACUC. Mice were housed in groups of no more than five per cage in facilities with controlled temperature and humidity with regulated light and dark cycles. Animals had free access to food and water.

Inducible *EGFR*$^{L858R}$ and *Twist1*/*EGFR*$^{L858R}$ transgenic mice in the FVB/N inbred background were of the genotype: CCSP-rtTA/tetO-*EGFR*$^{L858R}$ (CE) or CCSP-rtTA/tetO-*EGFR*$^{L858R}$/*Twist1*-tetO-luc (CET). The tetO-*EGFR*$^{L858R}$ mice were obtained from Dr. Katerina Politi (Yale University). All the mice were weaned at 3–4 weeks of age and then placed on doxycycline (DOX) drinking water at 4–8 weeks of age as previously described (24, 42). After three weeks of DOX treatment, CE and CET mice were randomized to vehicle and erlotinib treatment groups and stratifying by similar levels of tumor burden with micro-CT. Mice without tumor burden were excluded. These criteria were pre-established. Tumor burden was assessed by micro-CT imaging and quantitated as previously described (24). Evaluation of treatment response by microCT was blinded otherwise the identity of the animals were known to investigators.

Erlotinib was purchased from Selleckchem (Houston, TX). For *in vivo* experiments, erlotinib was dissolved into a slurry in 0.5% methylcellulose. The mice received 50 mg/kg erlotinib or vehicle via oral gavage 6 days a week for 3 weeks.

### Histology and immunohistochemistry

Tissues were fixed and subsequent histology and immunohistochemistry was performed as previously described (60). For immunohistochemistry, the primary antibodies were used at the following concentrations: Twist1 at 1:200, vimentin and e-cadherin at 1:400; cleaved caspase 3 at 1:500, and Ki-67 at 1:2000.

### Statistical analysis

Student t-test, ANOVA with Tukey's multiple comparison testing, and Mantel-Cox testing was performed where indicated. For transgenic animal studies, we used cohorts of >12 animals each. This was based on sample size calculations assuming experimental condition will result in animals that have a mean survival that is 45% longer than control treated mice with a power of 80% to detect a difference using the Kaplan-Meier long-rank test.

## Supplementary Material

Refer to Web version on PubMed Central for supplementary material.

## Acknowledgments:

This work was supported by the following funding sources: Dr. Hailun Wang has received research funding from the Uniting Against Lung Cancer Foundation. Dr. Burns was supported for this project from a V Foundation Scholar Award, American Lung Association Award (LCD 257864), Sidney Kimmel Foundation (SKF-15–099) and a Doris Duke Charitable Foundation Clinical Scientist Award (2015097), a Pittsburgh LUNG SPORE CDA P50CA090440 and generous support from the We Wish Foundation. This project used the Hillman Cancer Center Animal, Flow Cytometry and Biostatistics Facilities that are supported in part by award P30CA047904. Zachary Yochum has received research funding for this project from the Howard Hughes Medical Institute Medical

Fellowship, T32GM008421–22 and a 1F30CA213765–01. PT Tran research funding for this project from the Nesbitt Family; Movember-Prostate Cancer Foundation; Uniting Against Lung Cancer Foundation; American Lung Association (LCD-339465); Commonwealth Foundation; Sidney Kimmel Foundation (SKF-13–021); ACS (122688-RSG-12–196-01-TBG); DoD (W81XWH-13–1-0182); NIH/NCI (R01CA166348).

The authors thank Laura Stabile, PhD, James G. Herman, MD, and Frank P. Vendetti PhD at the University of Pittsburgh for the discussion, advice regarding experimental design and supply of reagents when applicable. In addition, we would like to acknowledge the helpful discussion and comments provided by the Burns, Rudin, and Tran laboratory members.

**Funding Sources:** This work was supported by the following funding sources: Dr. Hailun Wang has received research funding from the Uniting Against Lung Cancer Foundation. Dr. Burns was supported for this project from a V Foundation Scholar Award, American Lung Association Award (LCD 257864), Sidney Kimmel Foundation (SKF-15–099) and a Doris Duke Charitable Foundation Clinical Scientist Award (2015097), a Pittsburgh LUNG SPORE CDA P50CA090440 and generous support from the We Wish Foundation. This project used the Hillman Cancer Center Animal, Flow Cytometry and Biostatistics Facilities that are supported in part by award P30CA047904. Zachary Yochum has received research funding for this project from the Howard Hughes Medical Institute Medical Fellowship, T32GM008421–22 and a 1F30CA213765–01. PT Tran research funding for this project from the Nesbitt Family; Movember-Prostate Cancer Foundation; Uniting Against Lung Cancer Foundation; American Lung Association (LCD-339465); Commonwealth Foundation; Sidney Kimmel Foundation (SKF-13–021); ACS (122688-RSG-12–196-01-TBG); DoD (W81XWH-13–1-0182); NIH/NCI (R01CA166348).

## REFERENCES

1. The Cancer Genome Atlas Research N. Comprehensive molecular profiling of lung adenocarcinoma. Nature 2014;511(7511):543–50. [PubMed: 25079552]
2. Kris MG JB, Berry LD, Kwiatkowski DJ, Iafrate AJ, Wistuba II, Varella-Garcia M, et al. Using Multiplexed Assays of Oncogenic Drivers in Lung Cancers to Select Targeted Drugs. . JAMA 2014;311(19):1998–2006. [PubMed: 24846037]
3. Hirsch FR, Scagliotti GV, Mulshine JL, Kwon R, Curran WJ, Jr., Wu YL, et al. Lung cancer: current therapies and new targeted treatments. Lancet 2017;389(10066):299–311. [PubMed: 27574741]
4. Mok TS, Wu YL, Thongprasert S, Yang CH, Chu DT, Saijo N, et al. Gefitinib or carboplatin-paclitaxel in pulmonary adenocarcinoma. N Engl J Med 2009;361(10):947–57. [PubMed: 19692680]
5. Rosell R, Molina MA, Costa C, Simonetti S, Gimenez-Capitan A, Bertran-Alamillo J, et al. Pretreatment EGFR T790M mutation and BRCA1 mRNA expression in erlotinib-treated advanced non-small-cell lung cancer patients with EGFR mutations. Clin Cancer Res 2011;17(5):1160–8. [PubMed: 21233402]
6. Rosell R, Carcereny E, Gervais R, Vergnenegre A, Massuti B, Felip E, et al. Erlotinib versus standard chemotherapy as first-line treatment for European patients with advanced EGFR mutation-positive non-small-cell lung cancer (EURTAC): a multicentre, open-label, randomised phase 3 trial. Lancet Oncol 2012;13(3):239–46. [PubMed: 22285168]
7. Sequist LV, Waltman BA, Dias-Santagata D, Digumarthy S, Turke AB, Fidias P, et al. Genotypic and histological evolution of lung cancers acquiring resistance to EGFR inhibitors. Sci Transl Med 2011;3(75):75ra26.
8. Zhang Z, Lee JC, Lin L, Olivas V, Au V, LaFramboise T, et al. Activation of the AXL kinase causes resistance to EGFR-targeted therapy in lung cancer. Nat Genet 2012;44(8):852–60. [PubMed: 22751098]
9. Song KA, Niederst MJ, Lochmann TL, Hata AN, Kitai H, Ham J, et al. Epithelial-to-mesenchymal transition antagonizes response to targeted therapies in lung cancer by suppressing BIM. Clin Cancer Res 2017.
10. McGowan M, Kleinberg L, Halvorsen AR, Helland A, Brustugun OT. NSCLC depend upon YAP expression and nuclear localization after acquiring resistance to EGFR inhibitors. Genes Cancer 2017;8(3–4):497–504. [PubMed: 28680534]
11. Kalluri R, Weinberg RA. The basics of epithelial-mesenchymal transition. J Clin Invest 2009;119(6):1420–8. [PubMed: 19487818]
12. Thiery JP, Acloque H, Huang RY, Nieto MA. Epithelial-mesenchymal transitions in development and disease. Cell 2009;139(5):871–90. [PubMed: 19945376]

13. Byers LA, Diao L, Wang J, Saintigny P, Girard L, Peyton M, et al. An epithelial-mesenchymal transition gene signature predicts resistance to EGFR and PI3K inhibitors and identifies Axl as a therapeutic target for overcoming EGFR inhibitor resistance. Clin Cancer Res 2013;19(1):279–90. [PubMed: 23091115]
14. Suda K, Tomizawa K, Fujii M, Murakami H, Osada H, Maehara Y, et al. Epithelial to mesenchymal transition in an epidermal growth factor receptor-mutant lung cancer cell line with acquired resistance to erlotinib. J Thorac Oncol 2011;6(7):1152–61. [PubMed: 21597390]
15. Witta SE, Gemmill RM, Hirsch FR, Coldren CD, Hedman K, Ravdel L, et al. Restoring E-cadherin expression increases sensitivity to epidermal growth factor receptor inhibitors in lung cancer cell lines. Cancer Res 2006;66(2):944–50. [PubMed: 16424029]
16. Izumchenko E, Chang X, Michailidi C, Kagohara L, Ravi R, Paz K, et al. The TGFbeta-miR200-MIG6 pathway orchestrates the EMT-associated kinase switch that induces resistance to EGFR inhibitors. Cancer Res 2014;74(14):3995–4005. [PubMed: 24830724]
17. Jakobsen KR, Demuth C, Sorensen BS, Nielsen AL. The role of epithelial to mesenchymal transition in resistance to epidermal growth factor receptor tyrosine kinase inhibitors in non-small cell lung cancer. Transl Lung Cancer Res 2016;5(2):172–82. [PubMed: 27186512]
18. Vazquez-Martin A, Cufi S, Oliveras-Ferraros C, Torres-Garcia VZ, Corominas-Faja B, Cuyas E, et al. IGF-1R/epithelial-to-mesenchymal transition (EMT) crosstalk suppresses the erlotinib-sensitizing effect of EGFR exon 19 deletion mutations. Sci Rep 2013;3:2560. [PubMed: 23994953]
19. Yochum ZA, Socinski MA, Burns TF. Paradoxical functions of ZEB1 in EGFR-mutant lung cancer: tumor suppressor and driver of therapeutic resistance. J Thorac Dis 2016;8(11):E1528–E31. [PubMed: 28066651]
20. Yoshida T, Song L, Bai Y, Kinose F, Li J, Ohaegbulam KC, et al. ZEB1 Mediates Acquired Resistance to the Epidermal Growth Factor Receptor-Tyrosine Kinase Inhibitors in Non-Small Cell Lung Cancer. PLoS One 2016;11(1):e0147344. [PubMed: 26789630]
21. Zhang T, Guo L, Creighton CJ, Lu Q, Gibbons DL, Yi ES, et al. A genetic cell context-dependent role for ZEB1 in lung cancer. Nat Commun 2016;7:12231. [PubMed: 27456471]
22. Chang TH, Tsai MF, Su KY, Wu SG, Huang CP, Yu SL, et al. Slug confers resistance to the epidermal growth factor receptor tyrosine kinase inhibitor. Am J Respir Crit Care Med 2011;183(8):1071–9. [PubMed: 21037017]
23. Burns TF, Dobromilskaya I, Murphy SC, Gajula RP, Thiyagarajan S, Chatley SN, et al. Inhibition of TWIST1 leads to activation of oncogene-induced senescence in oncogene-driven non-small cell lung cancer. Mol Cancer Res 2013;11(4):329–38. [PubMed: 23364532]
24. Tran PT, Shroff EH, Burns TF, Thiyagarajan S, Das ST, Zabuawala T, et al. Twist1 suppresses senescence programs and thereby accelerates and maintains mutant Kras-induced lung tumorigenesis. PLoS Genet 2012;8(5):e1002650. [PubMed: 22654667]
25. Yochum ZA, Cades J, Mazzacurati L, Neumann NM, Khetarpal SK, Chatterjee S, et al. A First-in-Class TWIST1 Inhibitor with Activity in Oncogene-driven Lung Cancer. Mol Cancer Res 2017.
26. Yang J, Mani SA, Donaher JL, Ramaswamy S, Itzykson RA, Come C, et al. Twist, a master regulator of morphogenesis, plays an essential role in tumor metastasis. Cell 2004;117(7):927–39. [PubMed: 15210113]
27. Pham CG, Bubici C, Zazzeroni F, Knabb JR, Papa S, Kuntzen C, et al. Upregulation of Twist-1 by NF-kappaB blocks cytotoxicity induced by chemotherapeutic drugs. Mol Cell Biol 2007;27(11):3920–35. [PubMed: 17403902]
28. Cheng GZ, Chan J, Wang Q, Zhang W, Sun CD, Wang LH. Twist transcriptionally up-regulates AKT2 in breast cancer cells leading to increased migration, invasion, and resistance to paclitaxel. Cancer Res 2007;67(5):1979–87. [PubMed: 17332325]
29. Ansieau S, Bastid J, Doreau A, Morel AP, Bouchet BP, Thomas C, et al. Induction of EMT by twist proteins as a collateral effect of tumor-promoting inactivation of premature senescence. Cancer Cell 2008;14(1):79–89. [PubMed: 18598946]
30. Sos ML, Koker M, Weir BA, Heynck S, Rabinovsky R, Zander T, et al. PTEN loss contributes to erlotinib resistance in EGFR-mutant lung cancer by activation of Akt and EGFR. Cancer Res 2009;69(8):3256–61. [PubMed: 19351834]

31. Hwang W, Chiu YF, Kuo MH, Lee KL, Lee AC, Yu CC, et al. Expression of Neuroendocrine Factor VGF in Lung Cancer Cells Confers Resistance to EGFR Kinase Inhibitors and Triggers Epithelial-to-Mesenchymal Transition. Cancer Res 2017;77(11):3013–26. [PubMed: 28381546]
32. Jin HO, Hong SE, Woo SH, Lee JH, Choe TB, Kim EK, et al. Silencing of Twist1 sensitizes NSCLC cells to cisplatin via AMPK-activated mTOR inhibition. Cell Death Dis 2012;3:e319. [PubMed: 22673193]
33. Roberts CM, Tran MA, Pitruzzello MC, Wen W, Loeza J, Dellinger TH, et al. TWIST1 drives cisplatin resistance and cell survival in an ovarian cancer model, via upregulation of GAS6, L1CAM, and Akt signalling. Sci Rep 2016;6:37652. [PubMed: 27876874]
34. Zhuo WL, Wang Y, Zhuo XL, Zhang YS, Chen ZT. Short interfering RNA directed against TWIST, a novel zinc finger transcription factor, increases A549 cell sensitivity to cisplatin via MAPK/mitochondrial pathway. Biochem Bioph Res Co 2008;369(4):1098–102.
35. Faber AC, Corcoran RB, Ebi H, Sequist LV, Waltman BA, Chung E, et al. BIM expression in treatment-naive cancers predicts responsiveness to kinase inhibitors. Cancer Discov 2011;1(4): 352–65. [PubMed: 22145099]
36. Ohashi K, Sequist LV, Arcila ME, Moran T, Chmielecki J, Lin YL, et al. Lung cancers with acquired resistance to EGFR inhibitors occasionally harbor BRAF gene mutations but lack mutations in KRAS, NRAS, or MEK1. Proc Natl Acad Sci U S A 2012;109(31):E2127–33. [PubMed: 22773810]
37. Shi P, Oh YT, Deng L, Zhang G, Qian G, Zhang S, et al. Overcoming acquired resistance to AZD9291, a third generation EGFR inhibitor, through modulation of MEK/ERK-dependent Bim and Mcl-1 degradation. Clin Cancer Res 2017.
38. Costa DB, Halmos B, Kumar A, Schumer ST, Huberman MS, Boggon TJ, et al. BIM mediates EGFR tyrosine kinase inhibitor-induced apoptosis in lung cancers with oncogenic EGFR mutations. PLoS Med 2007;4(10):1669–79; discussion 1680. [PubMed: 17973572]
39. Deng J, Shimamura T, Perera S, Carlson NE, Cai D, Shapiro GI, et al. Proapoptotic BH3-only BCL-2 family protein BIM connects death signaling from epidermal growth factor receptor inhibition to the mitochondrion. Cancer Res 2007;67(24):11867–75. [PubMed: 18089817]
40. Sionov RV, Vlahopoulos SA, Granot Z. Regulation of Bim in Health and Disease. Oncotarget 2015;6(27):23058–134. [PubMed: 26405162]
41. Chang AT, Liu Y, Ayyanathan K, Benner C, Jiang Y, Prokop JW, et al. An evolutionarily conserved DNA architecture determines target specificity of the TWIST family bHLH transcription factors. Genes Dev 2015;29(6):603–16. [PubMed: 25762439]
42. Politi K, Zakowski MF, Fan PD, Schonfeld EA, Pao W, Varmus HE. Lung adenocarcinomas induced in mice by mutant EGF receptors found in human lung cancers respond to a tyrosine kinase inhibitor or to down-regulation of the receptors. Genes Dev 2006;20(11):1496–510. [PubMed: 16705038]
43. Zheng H, Kang Y. Multilayer control of the EMT master regulators. Oncogene 2014;33(14):1755–63. [PubMed: 23604123]
44. Soria JC, Ohe Y, Vansteenkiste J, Reungwetwattana T, Chewaskulyong B, Lee KH, et al. Osimertinib in Untreated EGFR-Mutated Advanced Non-Small-Cell Lung Cancer. N Engl J Med 2017.
45. Ramalingam SS, Yang JC, Lee CK, Kurata T, Kim DW, John T, et al. Osimertinib As First-Line Treatment of EGFR Mutation-Positive Advanced Non-Small-Cell Lung Cancer. J Clin Oncol 2017:JCO2017747576.
46. Ricordel C, Llamas-Gutierrez F, Chiforeanu D, Lena H, Corre R. Large Cell Neuroendocrine Lung Carcinoma Transformation as an Acquired Resistance Mechanism to Osimertinib. J Thorac Oncol 2017;12(11):e184–e6. [PubMed: 29074211]
47. Kim TM, Song A, Kim DW, Kim S, Ahn YO, Keam B, et al. Mechanisms of Acquired Resistance to AZD9291: A Mutation-Selective, Irreversible EGFR Inhibitor. J Thorac Oncol 2015;10(12): 1736–44. [PubMed: 26473643]
48. Eberlein CA, Stetson D, Markovets AA, Al-Kadhimi KJ, Lai Z, Fisher PR, et al. Acquired Resistance to the Mutant-Selective EGFR Inhibitor AZD9291 Is Associated with Increased

Dependence on RAS Signaling in Preclinical Models. Cancer Res 2015;75(12):2489–500. [PubMed: 25870145]

49. Planchard D, Loriot Y, Andre F, Gobert A, Auger N, Lacroix L, et al. EGFR-independent mechanisms of acquired resistance to AZD9291 in EGFR T790M-positive NSCLC patients. Ann Oncol 2015;26(10):2073–8. [PubMed: 26269204]
50. Ou SI, Agarwal N, Ali SM. High MET amplification level as a resistance mechanism to osimertinib (AZD9291) in a patient that symptomatically responded to crizotinib treatment post-osimertinib progression. Lung Cancer 2016;98:59–61. [PubMed: 27393507]
51. Li L, Wang H, Li C, Wang Z, Zhang P, Yan X. Transformation to small-cell carcinoma as an acquired resistance mechanism to AZD9291: A case report. Oncotarget 2017;8(11):18609–14. [PubMed: 28061471]
52. Moloudizargari M, Mikaili P, Aghajanshakeri S, Asghari MH, Shayegh J. Pharmacological and therapeutic effects of Peganum harmala and its main alkaloids. Pharmacogn Rev 2013;7(14):199–212. [PubMed: 24347928]
53. Borghaei H, Paz-Ares L, Horn L, Spigel DR, Steins M, Ready NE, et al. Nivolumab versus Docetaxel in Advanced Nonsquamous Non-Small-Cell Lung Cancer. N Engl J Med 2015;373(17): 1627–39. [PubMed: 26412456]
54. Tanimoto A, Takeuchi S, Arai S, Fukuda K, Yamada T, Roca X, et al. Histone Deacetylase 3 Inhibition Overcomes BIM Deletion Polymorphism-Mediated Osimertinib Resistance in EGFR-Mutant Lung Cancer. Clin Cancer Res 2017;23(12):3139–49. [PubMed: 27986747]
55. Soh SX, Siddiqui FJ, Allen JC, Kim GW, Lee JC, Yatabe Y, et al. A systematic review and meta-analysis of individual patient data on the impact of the BIM deletion polymorphism on treatment outcomes in epidermal growth factor receptor mutant lung cancer. Oncotarget 2017;8(25):41474–86. [PubMed: 28467813]
56. Jacqueroud L, Bouard C, Richard G, Payen L, Devouassoux-Shisheboran M, Spicer DB, et al. The Heterodimeric TWIST1-E12 Complex Drives the Oncogenic Potential of TWIST1 in Human Mammary Epithelial Cells. Neoplasia 2016;18(5):317–27. [PubMed: 27237323]
57. Pan D, Fujimoto M, Lopes A, Wang YX. Twist-1 is a PPARdelta-inducible, negative-feedback regulator of PGC-1alpha in brown fat metabolism. Cell 2009;137(1):73–86. [PubMed: 19345188]
58. Chen YT, Akinwunmi PO, Deng JM, Tam OH, Behringer RR. Generation of a Twist1 conditional null allele in the mouse. Genesis 2007;45(9):588–92. [PubMed: 17868088]
59. Moffat J, Grueneberg DA, Yang X, Kim SY, Kloepfer AM, Hinkle G, et al. A lentiviral RNAi library for human and mouse genes applied to an arrayed viral high-content screen. Cell 2006;124(6):1283–98. [PubMed: 16564017]
60. Tran PT, Bendapudi PK, Lin HJ, Choi P, Koh S, Chen J, et al. Survival and Death Signals Can Predict Tumor Response to Therapy After Oncogene Inactivation. Science Translational Medicine 2011;3(103).

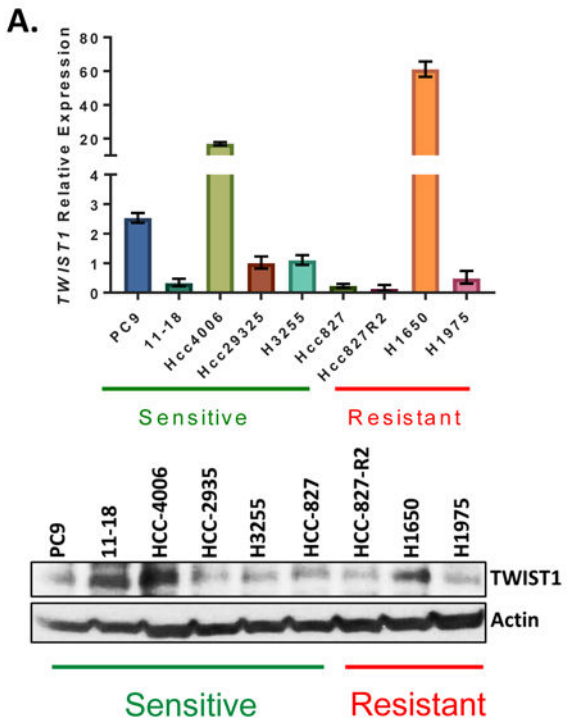


| Cell Line | EGFR mutation |
|---|---|
| PC9 | E746-A750del |
| 11-18 | L858R |
| Hcc4006 | L747-E749del |
| Hcc2935 | E746-751Tdel |
| H3255 | L858R |
| Hcc827 | E746-A750del |
| Hcc4011 | L858R |
| H1650 | E746-A750del |
| H1975 | T790M, L858R |

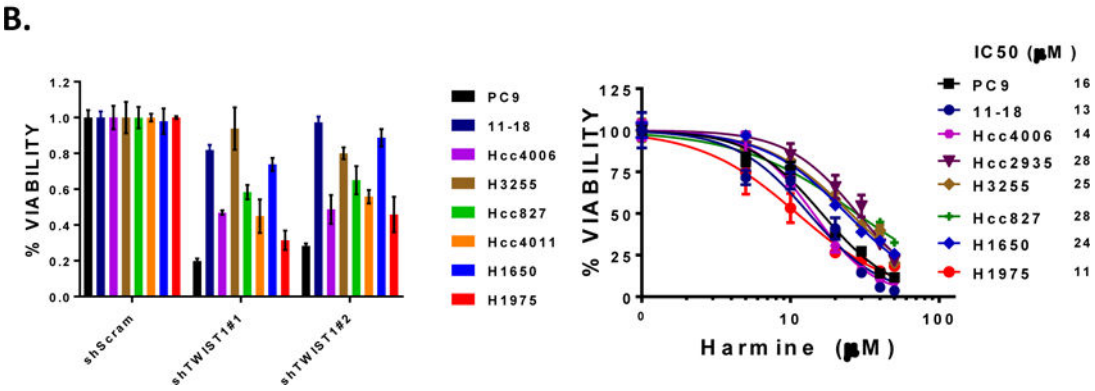


**Figure 1: TWIST1 is required for *EGFR*-mutant NSCLC.**

**(A) LEFT:** Quantitative RT-PCR demonstrating baseline *TWIST1* mRNA (TOP) and protein (BOTTOM) levels in a panel of erlotinib sensitive and resistant *EGFR*-mutant NSCLC cells. RT-PCR was normalized to Hcc2935 mRNA levels. Data represent mean ±SD (n=3 technical replicates). RIGHT: Chart demonstrating EGFR-mutations in the NSCLC cell lines utilized. EGFR TKI sensitive cells are colored in green and EGFR TKI resistant cells are colored in red. **(B)** LEFT: Cell-Titer Glo assays demonstrating that knockdown of TWIST1 results in growth inhibition in a panel of *EGFR*-mutant NSCLC cell lines. Cells were infected with shScram or shRNA targeting *TWIST1* (shTWIST1 #1, #2) for 6 days. Viability data was normalized to shScram control. Data represent mean ± SD (n=4 technical replicates). RIGHT: MTS assays demonstrating that harmine has activity in a panel of *EGFR*-mutant NSCLC cells. Cells were treated with harmine for 72 hours. Data represent mean ± SD (n=4 technical replicates).

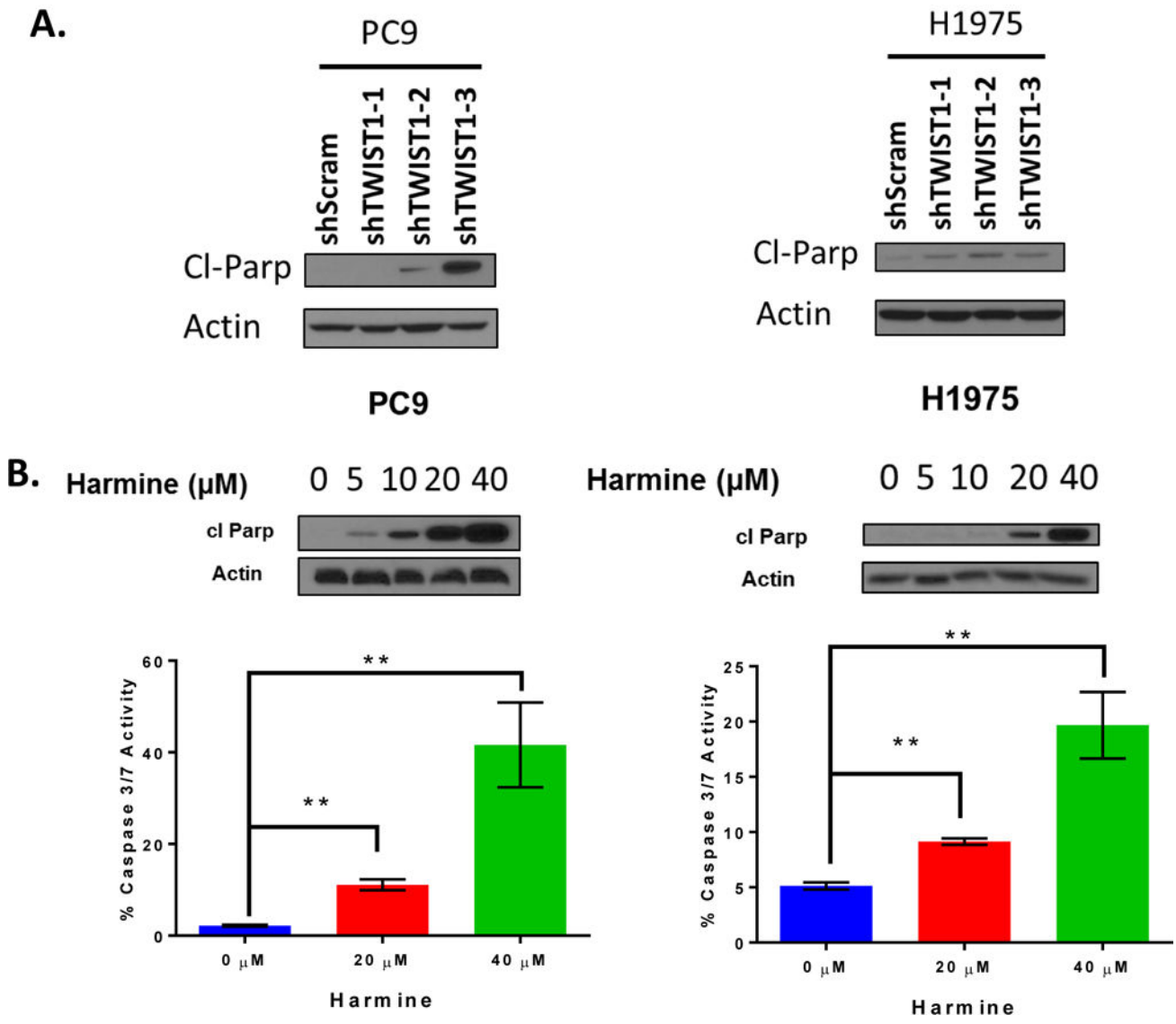


**Figure 2: Inhibition of TWIST1 results in apoptosis in a subset of *EGFR*-mutant NSCLC cell lines**

**(A)** Western blot demonstrating that knockdown of TWIST1 induces apoptosis in PC9 cells with EGFR TKI sensitizing *EGFR* exon 19 deletion (ΔE746-A750) and H1975 cells with both EGFR TKI sensitizing *L858R* mutation and an acquired resistance *T790M* mutation. Cells were infected with shScram and shRNA targeting *TWIST1* (shTWIST1 #1–3) for 72 hours (PC9) or 6 days (H1975) and harvested for Western blot. **(B)** UPPER: Western blots demonstrating that harmine treatment results in PARP cleaved in PC9 and H1975 cells. Cells were treated with harmine for 48 hours and harvested for Western blot analysis. LOWER: Active Caspase 3–7 staining demonstrating induction of apoptosis in PC9 and H1975 following 48 hours of harmine treatment. Data represents mean ± SD (n=3 biological replicates). **, p<.01, 2-tailed Student's t-test.

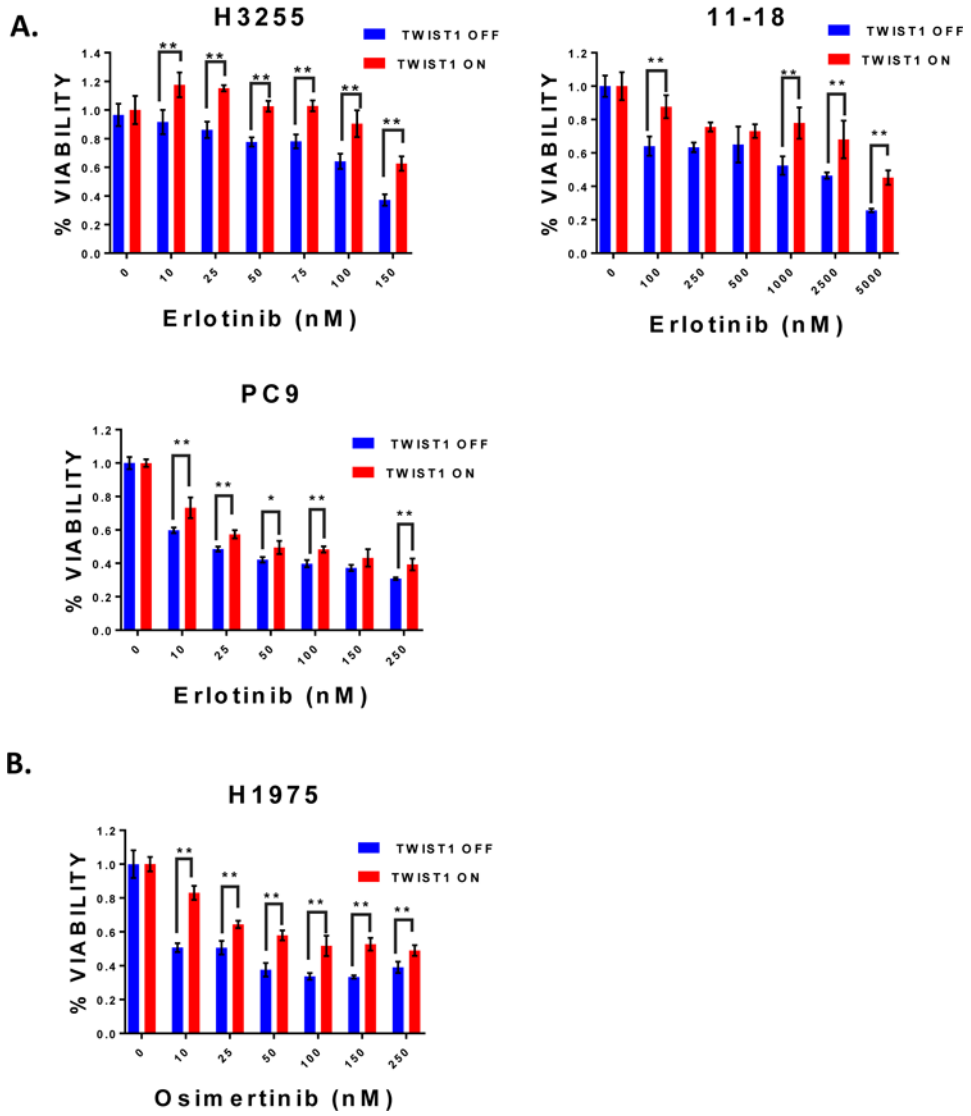


**Figure 3: TWIST1 overexpression is sufficient to mediate resistance to EGFR TKIs.**

**(A)** UPPER: MTS or Cell-Titer Glo assays demonstrating that TWIST1 overexpression results in decreased response to erlotinib. H3255 TRE3G-TWIST1 (UPPER LEFT), 11–18 TRE3G-TWIST1 (UPPER RIGHT), and PC9 TRE3G-TWIST1 (LOWER) were pre-treated with doxycycline for 72 hours and then treated with doxycycline and erlotinib for 72 hours. Data represent mean ± SD (n=4 technical replicates). *, P<.05, **, P<.01, 2-way ANOVA, followed by Tukey's Test. **(B)** MTS assay demonstrate that TWIST1 overexpression decreases response to osimertinib. H1975 TRE3G-TWIST1 were pre-treated with doxycycline for 72 hours prior to a 72 hour treatment with osimertinib. Data represent mean ± SD (n=4 technical replicates). *, P<.05, **, P<.01, 2-way ANOVA, followed by Tukey's Test.

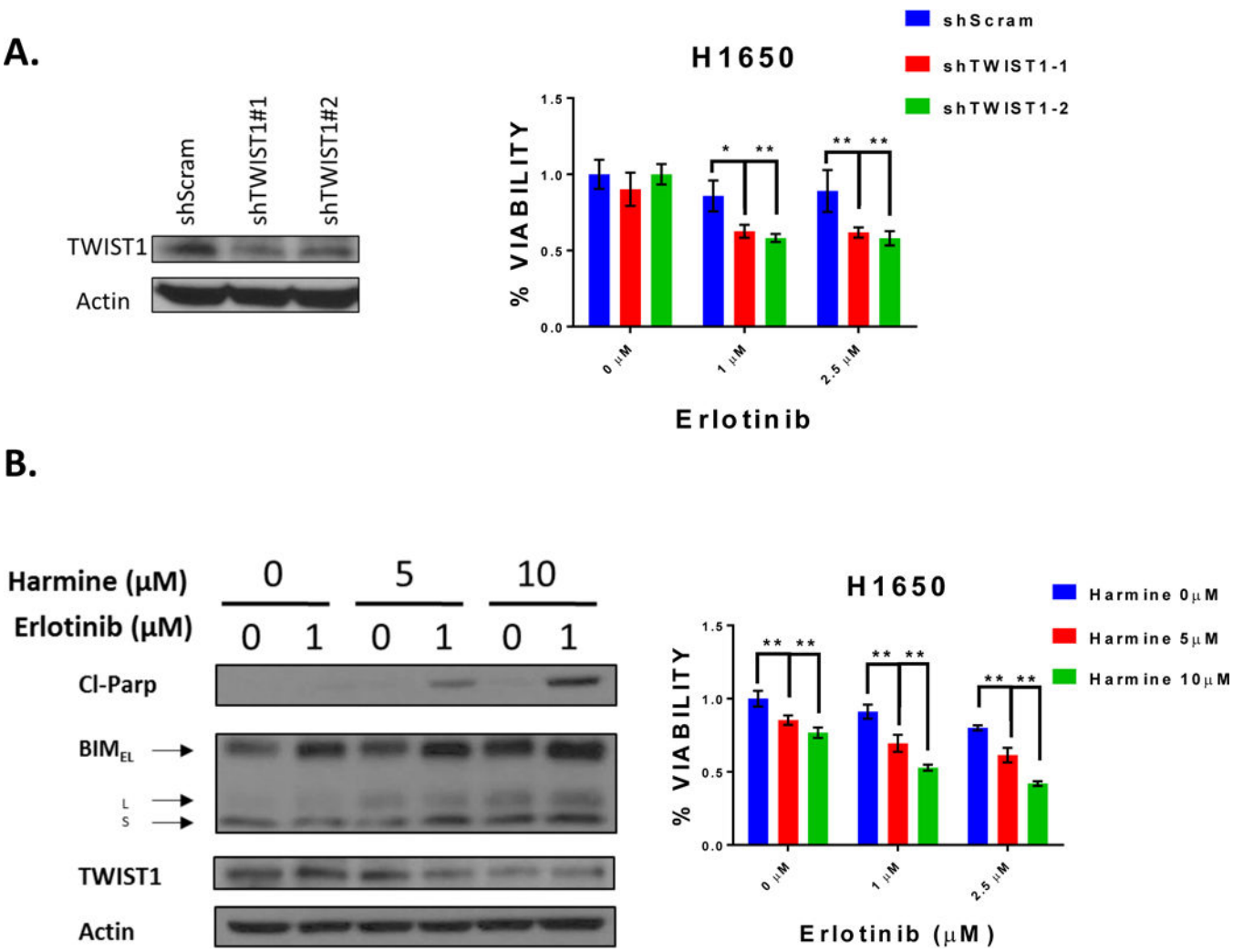


**Figure 4: Inhibition of TWIST1 is sufficient to overcome EGFR TKI resistance.**

**(A)** LEFT: Western blot demonstrating shRNA targeting TWIST1 decreases TWIST1 levels. The erlotinib resistant cell line, H1650 was infected with the indicated shRNA and harvested six days following infection for Western analysis. RIGHT: MTS assay demonstrating that knockdown of *TWIST1* in H1650 cells can re-sensitize cells to erlotinib. H1650 cells which harbor both *EGFR* and *PTEN* mutations, were infected with the indicated shRNAs for 48 hours and subsequently treated with erlotinib for 72 hours. Data represent mean ±SD (n=4 technical replicates). *, P<.05, **, P<.01, 2-way ANOVA, followed by Tukey's Test. **(B)** LEFT: Western blot demonstrating that the combination of harmine and erlotinib results in increased apoptosis as measured by PARP cleavage as well as BIM expression, and decreased TWIST1 expression. H1650 cells were treated with the indicated doses of harmine and erlotinib for 48 hours and harvested for Western analysis. RIGHT: MTS assay demonstrating that harmine treatment increases H1650 cell sensitivity to erlotinib. Cells were treated with the indicated doses of harmine and erlotinib for 48 hours. Data represent

mean ±SD (n=4 technical replicates). *, P<.05, **, P<.01, 2-way ANOVA, followed by Tukey's Test.

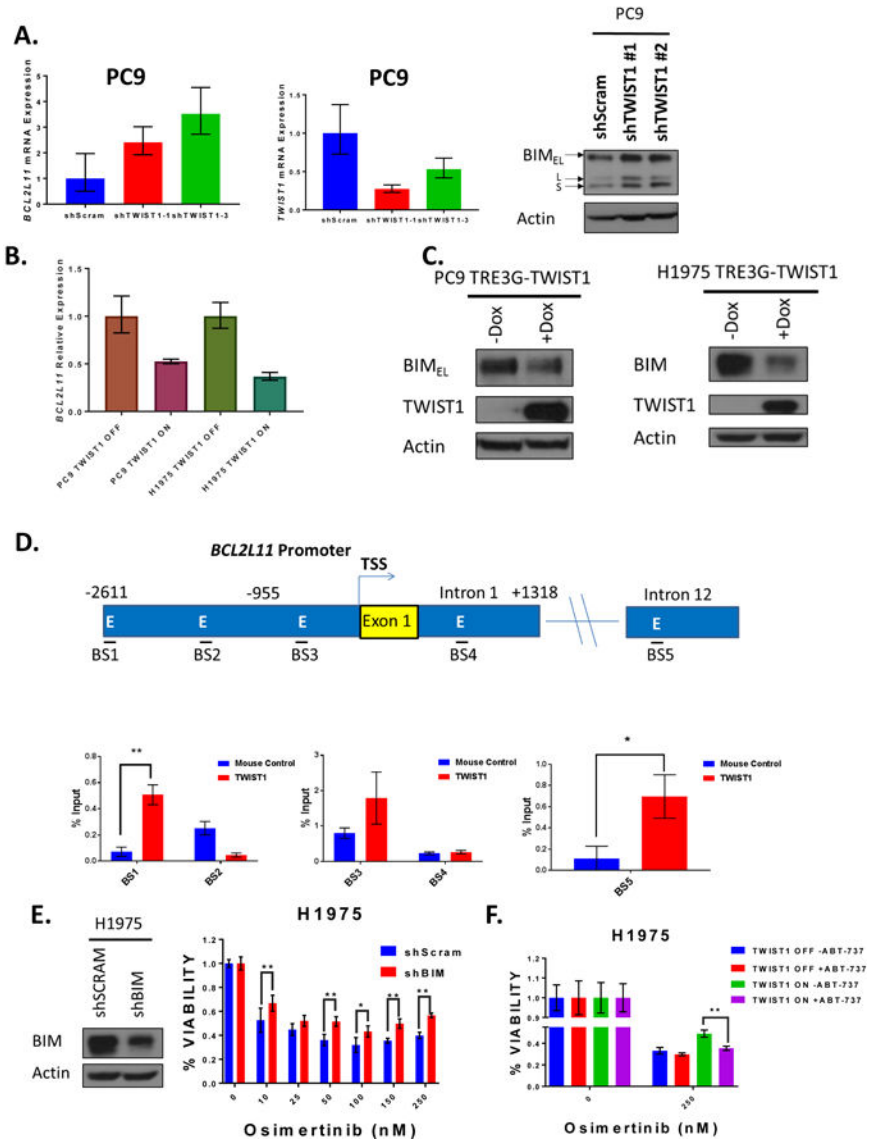


**Figure 5: TWIST1 suppresses BIM expression.**

**(A)** LEFT: Quantitative RT-PCR (qRT-PCR) demonstrating increased *BCL2L11* mRNA levels following knockdown of TWIST1. PC9 cells were infected with the indicated shRNA for 24 hours. Data represent mean ±SD (n=3 technical replicates). RIGHT: Western blot demonstrating that knockdown of *TWIST1* increased BIM protein levels. PC9 cells were infected with the indicated shRNA for 72 hours. **(B)** qRT-PCR demonstrating that TWIST1 overexpression decreased *BCL2L11* mRNA levels. PC9 TRE3G-TWIST1 cells and H1975 TRE3G-TWIST1 were treated with doxycycline for 24 hours. Data represent mean ±SD (n=3 technical replicates). **(C)** Western blot demonstrating that TWIST1 overexpression decreased BIM protein levels. PC9 TRE3G-TWIST1 cells and H1975 TRE3G-TWIST1 were treated with doxycycline for 72 hours. **(D)** ChIP assay demonstrating TWIST1 binding to promoter and intronic regions of *BCL2L11*. UPPER: Model demonstrating E-box sites within the *BCL2L11* promoter, Intron 1, and Intron 12 that were interrogated for TWIST1

binding. LOWER: qRT-PCR demonstrating that TWIST1 is enriched at multiple sites within the *BCL2L11* promoter and intronic regions. Data represent mean ±SD (n=3 technical replicates). *, P<.05, **, P<.01. 2-tailed Student's t-test. **(E)** LEFT: Western blot demonstrating that shRNA targeting BIM decreased BIM expression. RIGHT: MTS assay demonstrating decreased response to osimertinib following knockdown of BIM in H1975 cells. H1975 cells that stably express shScram or shBIM were treated with osimertinib for 72 hours. Data represent mean ±SD (n=4 technical replicates). *, P<.05, **, P<.01, 2-way ANOVA, followed by Tukey's Test. **(F)** MTS assay demonstrating that TWIST1-mediated resistance to osimertinib can be overcome with ABT-737. H1975 TRE3G-TWIST1 cells were pre-treated with doxycycline for 72 hours and then co-treated with osimertinib and ABT-737 (1μM) ± doxycycline for 72 hours. Data represent mean ±SD (n=4 technical replicates). **, P<.01, 2-way ANOVA, followed by Tukey's Test.

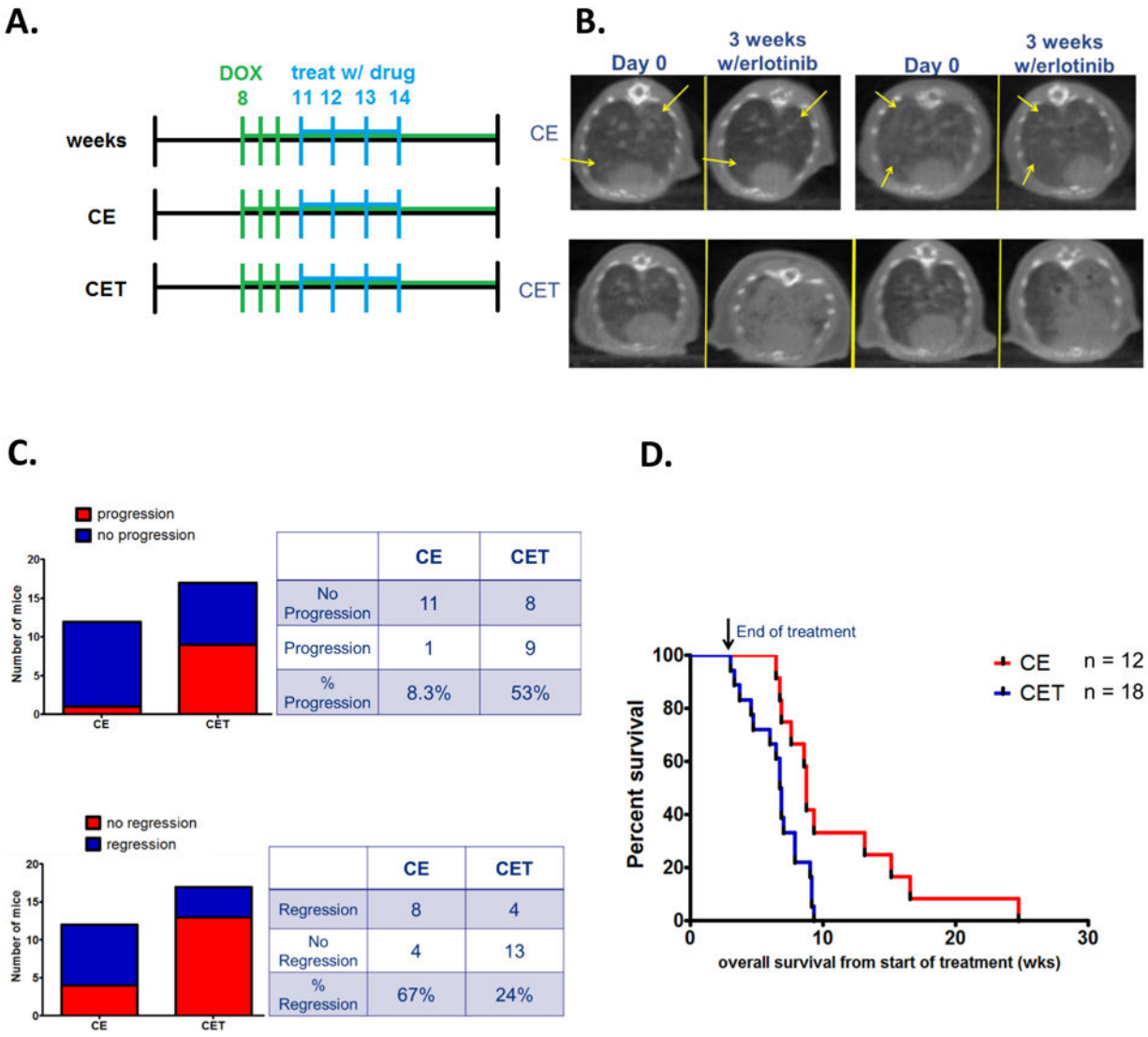


**Figure 6: Twist1 overexpression *in vivo* is sufficient to cause erlotinib resistance.**

**(A)** Treatment schema for CE and CET mice erlotinib treatment. Mice were started on doxycycline, inducing $EGFR^{L858R}$ and *Twist1* transgene expression, at 8 weeks of age and allowed to develop tumors for 3 weeks prior to erlotinib treatment. Mice were scanned at the beginning of treatment, week 11, and each week thereafter until the end of treatment. Mice are treated with 50 mg/kg erlotinib by oral gavage 6 days a week for 3 weeks (weeks 11–14). **(B)** Representative CT images from baseline and after 3 weeks of erlotinib treatment for CE and CET mice. CE mice show a decrease in tumor burden at the end of treatment compared to day 0. CET mice show a drastic increase in tumor burden despite 3 weeks of treatment. **(C)** Tumor burden, as visualized by CT image, was graded on a scale of 0 (no tumor) to 5 (lungs filled with tumor) at day 0 and the end of treatment. No progression was considered a complete or partial response as well as stable disease. Only 1 CE mouse demonstrated disease progression, while over half of the CET mice progressed despite erlotinib treatment. Regression was a decrease in tumor burden grade at 3 weeks compared

to baseline. Two-thirds of CE mice regressed, while only one quarter of CET mice showed regression. **(D)** Kaplan-Meier overall survival from beginning of treatment. Median survival for CE mice was 8.7 weeks, for CET mice was 6.8 weeks. Difference in survival was statistically significant using the Mantel Cox test, P=0.0073.

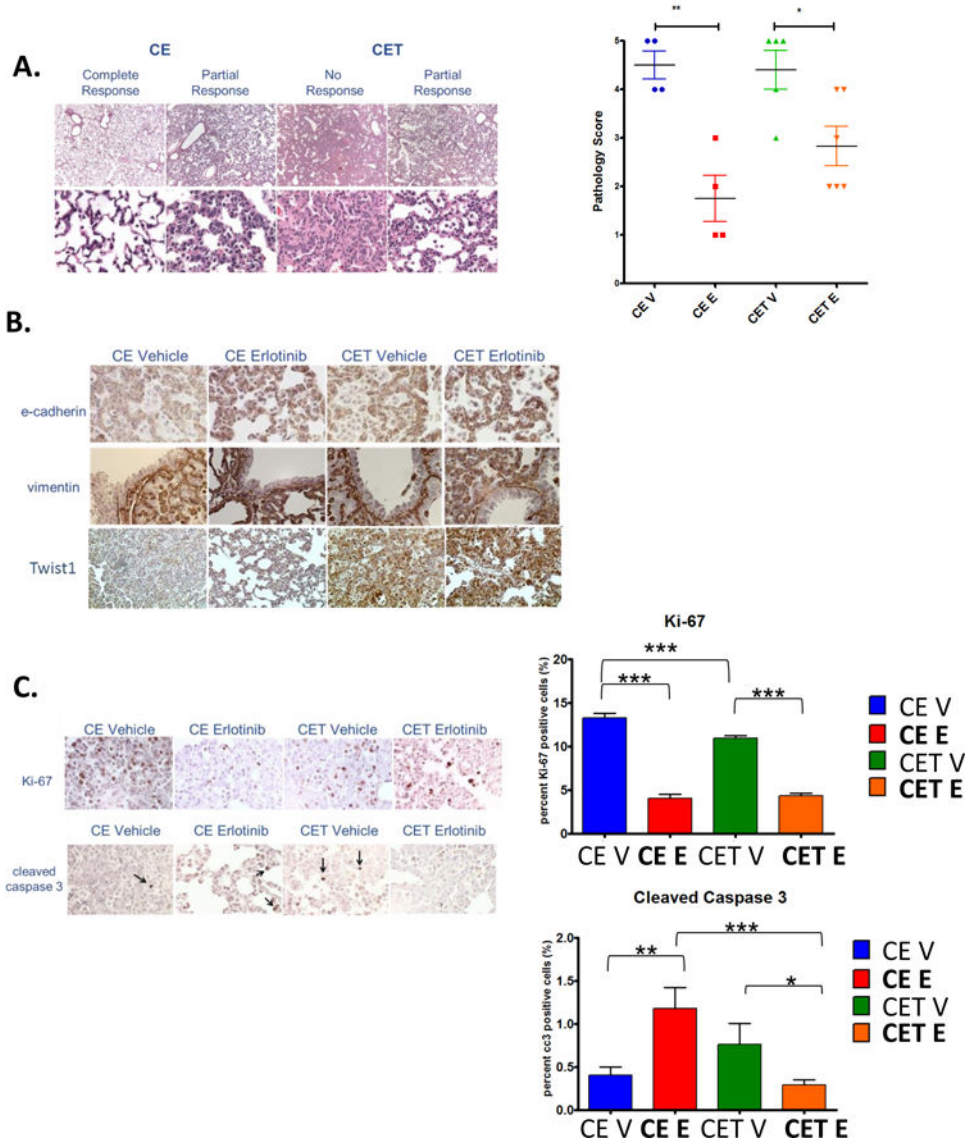


**Figure 7: Characterization of TWIST1-mediated erlotinib resistance *in vivo*.**

**(A)** LEFT: H&E images showing comparison of responses seen in CE and CET mice after 7 days of erlotinib treatment. Black bars equal 500 (top) and 50 (bottom) μm. RIGHT: Pathology scores indicating tumor burden as percent of total lung affected. **(B)** Similar levels of E-cadherin and vimentin staining in CE and CET mice with and without erlotinib treatment, with CET mice expressing Twist1. **(C)** LEFT: Representative images of Ki-67 and cleaved caspase 3 staining and quantification (RIGHT) of staining showing a decrease in proliferation to similar levels with erlotinib treatment in both CE and CET mice and a decrease in apoptosis in CET compared to CE mice following erlotinib treatment. Differences were statistically significant using Student t-test, * $p<0.05$, ** $p<0.005$, *** $p<0.0005$.